Contract No. and Disclaimer:

This manuscript has been authored by Savannah River Nuclear Solutions, LLC under Contract No. DE-AC09-08SR22470 with the U.S. Department of Energy. The United States Government retains and the publisher, by accepting this article for publication, acknowledges that the United States Government retains a non-exclusive, paid-up, irrevocable, worldwide license to publish or reproduce the published form of this work, or allow others to do so, for United States Government purposes.

Application Note:

Use of Atomic Layer Deposition of Functionalization of Nanoporous Biomaterials

Roger J Narayan[1], Shashishekar P Adiga[2], Michael J Pellin[3],
Larry A Curtiss[3], Shane Stafslien[4], Bret Chisholm[4],
Nancy A Monteiro-Riviere[1,5], Robin L Brigmon[6], Jeffrey W Elam[7]

[1]Joint Department of Biomedical Engineering, University of North Carolina and North Carolina State University, 2147 Burlington Engineering Labs, Raleigh NC 27695-7115 USA

[2]Kodak Research Laboratories, Eastman Kodak Company, Rochester, NY 14650 USA

[3]Materials Science Division, Argonne National Laboratory, Argonne, IL 60439 USA

[4]Center for Nanoscale Science and Engineering, North Dakota State University, 1805 Research Park Drive, Fargo, ND, 58102, USA

[5]Center for Chemical Toxicology Research and Pharmacokinetics, North Carolina State University, Raleigh, NC 27606 USA

[6]Savannah River National Laboratory, Aiken, SC, 29808 USA

[7]Energy Science Division, Argonne National Laboratory, Argonne, IL 60439 USA

Corresponding author

Roger J. Narayan

Joint Department of Biomedical Engineering

University of North Carolina and North Carolina State University

Raleigh, NC 27695-7115

Telephone: (919) 696-8488

Fax: (919) 513-3814

Email: roger_narayan@msn.com

Abstract

Due to its chemical stability, uniform pore size, and high pore density, nanoporous alumina is being investigated for use in biosensing, drug delivery, hemodialysis, and other medical applications. In recent work, we have examined the use of atomic layer deposition for coating the surfaces of nanoporous alumina membranes. Zinc oxide coatings were deposited on nanoporous alumina membranes using atomic layer deposition. The zinc oxide-coated nanoporous alumina membranes demonstrated antimicrobial activity against *Escherichia coli* and *Staphylococcus aureus* bacteria. These results suggest that atomic layer deposition is an attractive technique for modifying the surfaces of nanoporous alumina membranes and other nanostructured biomaterials.

Keywords

aluminum oxide, atomic layer deposition, biomaterial, nanomaterial, zinc oxide

Manuscript Body

Nanoporous alumina, also known as anodic aluminum oxide (AAO), is a nanomaterial that exhibits several unusual properties, including high pore densities, straight pores, small pore sizes, and uniform pore sizes.[1] In 1953, Keller et al. showed that anodizing aluminum in acid electrolytes results in a thick layer of nearly cylindrical pores, which are arranged in a close-packed hexagonal cell structure.[2] More recently, Matsuda & Fukuda demonstrated preparation of highly ordered platinum and gold nanohole arrays using a replication process. In this study, a negative structure of nanoporous alumina was initially fabricated and a positive structure of a nanoporous metal was subsequently fabricated.[3] Over the past fifteen years, nanoporous alumina membranes have been used as templates for growth of a variety of nanostructured materials, including nanotubes, nanowires, nanorods, and nanoporous membranes.[4,5, 6]

Nanoporous alumina membranes have also been considered for use in a variety of medical devices. Alumina is generally considered to be a biologically inert material; unlike nanoporous silicon, it does not induce calcium phosphate deposition or undergo biodegradation. [7, 8, 9, 10] For example, Gong et al. evaluated diffusion of fluorescein isothiocyanate and dextran conjugates from nanoporous alumina capsules; the capsules prevented transport of molecules larger than a given size.[11] Orosz et al. demonstrated use of nanoporous alumina for delivery of angiostatic and antioxidant pharmacologic agents, including catalase, endostatin, and vitamin C.[12] Darder et al. fabricated an amperometric glucose oxidase biosensor, which contained a nanoporous alumina membrane.[13] La Flamme et al. developed immunoisolation devices out of nanoporous alumina and poly(ethylene glycol)-modified nanoporous alumina; these materials were shown to be nontoxic and did not initiate significant complement activation.[14] Poly(ethylene glycol)-modified nanoporous alumina demonstrated fewer interactions with serum albumin than unmodified nanoporous alumina. Attaluri et al. considered the use of nanoporous alumina membranes for hemodialysis; no albumin leakage was noted from the nanoporous alumina membranes.[15] They demonstrated that the hydraulic conductivity of nanoporous alumina exceeded that of polyethersulfone. In a recent study, Graham et al. evaluated the interface between neuronal cells and nanoporous alumina electrodes.[16] They demonstrated growth of murine neuroblastoma glioma hybrid cells on nanoporous alumina.

In recent work, we have evaluated the use of a thin film growth process known as atomic layer deposition for depositing metallic and ceramic coatings on nanoporous alumina membranes. In atomic layer deposition, alternating chemical reactions between gaseous precursor molecules take place on a surface of a material.[17] Self-terminating gas-solid reactions allow for deposition of material in a layer-by-layer fashion. Reactions are

separated by purge steps, which involve saturation with an inert gas. Since the substrate is saturated during each reaction, atomic layer deposition may be used to deposit conformal coatings on nanoporous materials and other materials with high aspect ratio features.[18, 19]

Atomic layer deposition may be utilized to modify the surface properties of nanoporous alumina membranes used in biomedical applications. Xiong et al. suggested that impurities are incorporated within nanoporous alumina membranes during membrane synthesis; these impurities could alter the chemical and biological properties of the membranes.[17] Atomic layer deposition may be used to prevent release of these impurities. In addition, atomic layer deposition may be used to decrease the sizes of the pores within nanoporous alumina membranes in a controlled manner.[20] Adiga et al. demonstrated that a PEGylated platinum-coated nanoporous alumina membrane, which was prepared by atomic layer deposition of platinum and self-assembly of 1-mercaptoundec-11-yl hexa(ethylene glycol) on a nanoporous alumina membrane, remained free of protein adsorption and platelet aggregation after exposure to human platelet rich plasma.[1] Narayan et al. deposited titanium oxide coatings onto nanoporous alumina membranes using atomic layer deposition; titanium oxide-coated 20 nm pore size nanoporous alumina membranes exposed to ultraviolet light were shown to exhibit antimicrobial activity against two pathogenic microorganisms, *Escherichia coli* and *Staphylococcus aureus*.[21] Moon et al. reduced the pore size of nanoporous alumina membranes by means of atomic layer deposition.[22] Bacteriophage phi29 virus nanoparticles were subsequently aligned in the pores of the nanoporous alumina membranes using centrifugation; selective filtration of nanoparticles was demonstrated. Velleman et al. deposited silica coatings on nanoporous alumina membranes using atomic layer deposition; they subsequently modified the silica-coated membranes with perfluorodecyldimethylchlorosilane.[23] These hydrophobic membranes exhibited enhanced transport of hydrophobic agents (e.g., tris(2,2′-bipyridyl)dichlororuthenium(II) hexahydrate) over hydrophilic ones (e.g., Rose Bengal). In recent work, Narayan et al. deposited zinc oxide coatings on 100 nm pore size nanoporous alumina membranes using atomic layer deposition.[24] Scanning electron microscopy revealed that the inner surfaces of the membrane pores were completely coated with 5-10 nm zinc oxide nanocrystals. Energy dispersive X-ray analysis of a cleaved zinc oxide-coated nanoporous alumina membrane indicated that the zinc oxide concentration was uniform throughout. X-ray diffraction of the zinc oxide-coated nanoporous alumina indicated the presence of hexagonal zincite. The zinc oxide-coated membranes demonstrated activity against *Escherichia coli* and *Staphylococcus aureus* bacteria in agar diffusion assays.

In this study, the use of atomic layer deposition for coating surfaces of commercially-obtained 20 nm pore size nanoporous alumina membranes with zinc oxide is demonstrated. Human epithelial keratinocyte viability on the

zinc oxide-coated nanoporous alumina membranes was examined using a 3-(4,5-dimethylthiazol-2-yl)2,5-diphenyl tetrazolium bromide (MTT) assay. Microbial growth on the zinc oxide-coated nanoporous alumina membranes was determined using in vitro assays.

Atomic layer deposition was used to deposit zinc oxide coatings on 20 nm pore size nanoporous alumina membranes (Whatman, Maidstone, United Kingdom); these membranes exhibited thicknesses of 60 μm. Pores with diameters of 200 nm were observed over ~58 μm of the membrane thickness. The pores tapered to diameters of 20 nm over ~2 μm of the membrane thickness. The membranes were initially cleaned in situ using a five minute exposure to flowing ozone; an ozone partial pressure of ~0.1 Torr was obtained using ultrahigh purity oxygen (flow rate=400 sccm). Atomic layer deposition of zinc oxide coatings on nanoporous alumona membranes was performed using alternating exposure to water and diethyl zinc (Sigma Aldrich, St. Louis, United States). A deposition temperature of 200° C was used in this study. Thirty-one atomic layer deposition cycles were performed; precursor exposure times and precursor partial pressures of six seconds and ~0.2 Torr were utilized, respectively. Five second purge periods were used to separate precursor exposures. Ellipsometry of the Si(100) witness samples, which were coated at the same time as the nanoporous alumina membranes, yielded zinc oxide coating thicknesses of 5-6 nm. Uncoated and zinc oxide-coated nanoporous alumina membranes were imaged using a 3200 scanning electron microscope (Hitachi, Tokyo, Japan). Figure 1 shows a plan-view scanning electron micrograph of the large pore side of a zinc oxide-coated 20 nm pore size nanoporous alumina membrane; the pores exhibited relatively uniformly sizes. X-ray photoelectron spectra were obtained from zinc oxide-coated and uncoated nanoporous membranes using an LAS-3000 instrument (Riber, Bezons, France) with a Mg K□ anode source; the characteristic 2p peak for aluminum was not observed in the spectrum of the zinc oxide-coated membrane. CasaXPS software (RBD Instruments, Bend, United States) confirmed the absence of surface aluminum in the zinc oxide-coated membrane.

We examined the proliferation of neonatal human epidermal keratinocytes on zinc oxide-coated and uncoated 20 nm pore size nanoporous alumina membranes using the MTT assay, which involves the reduction of a yellow tetrazolium salt (MTT) to a purple formazan dye by mitochondrial succinic dehydrogenase.[21, 24] Three uncoated membranes and three zinc oxide-coated membranes were examined in this study. The uncoated and coated membranes were sterilized using ultraviolet B light; the membranes were exposed for three hours on each side and rotated 90° every forty-five minutes. The membranes were subsequently placed in twenty-four well plates. A small drop of Akwa Tears® (Akorn, Lake Forest, United States) was placed on the bottom of each well in order to prevent floating of the membranes. The wells and membranes were rinsed with 1 ml of keratinocyte growth medium-2 and were then seeded with 25,000 human epidermal keratinocytes in 1 ml of

keratinocyte growth medium-2 per well. The media was changed after twenty-four hours. After the cells were 60% confluent, they were grown for twenty-four hours. The membranes were moved to new twenty-four well plates to prevent cell growth outside the membranes from influencing the data. The data for the zinc oxide-coated membranes was standardized to the data for the uncoated membranes. Twenty-four hour MTT viability assay data for the uncoated 20 nm pore size nanoporous alumina membrane and the zinc oxide-coated 20 nm pore size nanoporous alumina membrane are shown in Figure 2; the zinc oxide-coated membrane exhibited higher viability than the uncoated membrane. Naji and Harmand previously demonstrated the cytocompatibility of amorphous alumina using in vitro assays.[25] The increase in cell proliferation on zinc oxide-coated membranes may be attributed to activation of mitogen-activated protein kinase and promotion of DNA synthesis by zinc.[26, 27]

Staphylococcus aureus ATCC 29213 and *Escherichia coli* ATCC 25922 (American Type Culture Collection, Manassas, United States) were used to examine the antimicrobial properties of zinc oxide-coated and uncoated nanoporous alumina membranes. The zinc oxide-coated membranes and uncoated membranes were sterilized by autoclaving prior to testing. The bacteria were cultured overnight to log phase in tryptic soy broth (Difco, Detroit, United States) within a shaking incubator (temperature=25° C). The *Staphylococcus aureus* and *Escherichia coli* cultures were subsequently washed three times with 0.2 μm filter-sterilized 0.1 M phosphate buffered saline. The cell densities of *Staphylococcus aureus* and *Escherichia coli* were brought to 10^7 cell/L and examined using a spectrophotometer before testing. Zinc oxide-coated and uncoated membranes were mounted on sterile microscope slides with autoclaved stainless steel clips. Slides containing the membranes were separately placed in sterile Petri dishes, which were covered with 20 ml of *Staphylococcus aureus* or *Escherichia coli* in phosphate-buffered saline solution. A control set of zinc oxide-coated membranes and uncoated membranes was treated with uninoculated phosphate-buffered saline solution. All of the Petri dishes were placed on a shaker table and incubated for four hours at 25° C. The Petri dishes were subsequently removed from the incubator. All of the membranes were rinsed three times with phosphate-buffered saline in order to remove unattached bacteria. Slides containing the washed membranes were air dried in a sterile hood, stained with fluorescein isothiocyanate (FITC) for ten minutes, and washed three times with filter-sterilized (0.2 μm) deionized water. The membranes were observed with fluorescence microscopy using a Model 510 laser scanning confocal microscope (Carl Zeiss, Thornwood, United States). *Staphylococcus aureus* attachment and growth on the uncoated membrane (Figure 3(a)) was approximately ten times greater than that on the zinc oxide-coated membrane (Figure 3(b)). A biofilm as well as colonies of *Staphylococcus aureus* were observed in Figure 3(a). *Escherichia coli* attachment and growth on the uncoated nanoporous alumina membrane (Figure 3(c)) was approximately three times greater than that on the zinc oxide-coated membrane (Figure 3(d)). It was

noted on that some of the *Escherichia coli* on the uncoated slide did not stain very well (Figure 3(c)); this lack of staining by fluorescein isothiocyanate may be attributed to the presence of a microbial biofilm. The control membranes, which were covered with uninoculated phosphate-buffered saline, showed no evidence of microbial colonization.

Microbial growth on zinc oxide-coated and uncoated membranes was also evaluated using an agar plating assay. Luria-Bertani broth, Luria-Bertani agar, 10 X phosphate-buffered saline, tryptic soy broth, tryptic soy agar, and triphenyltetrazolium chloride, were obtained from a commercial source (VWR International, West Chester, United States). 1 X phosphate-buffered saline was prepared using deionized water. Overnight cultures of *Staphylococcus aureus* ATCC 25923 (American Type Culture Collection, Manassas, United States) in tryptic soy broth and *Escherichia coli* ATCC 12435 (American Type Culture Collection, Manassas, United States) in Luria-Bertani broth were pelleted by means of centrifugation (speed=4500 rpm) for ten minutes. The microorganisms were resuspended in phosphate-buffered saline to prepare a final cell density of ~10^8 cells $ml^{-1.}$ Lawns of *Staphylococcus aureus* were inoculated on tryptic soy agar plates and lawns of *Escherichia coli* were inoculated on Luria-Bertani agar plates using sterile swabs. Zinc oxide-coated membranes and uncoated membranes were placed on these plates. One set of plates was inverted and incubated for twenty-four hours at 37° C in the dark. An additional set of plates was incubated under continuous exposure to a tungsten-halogen light source, which was located in the incubator. The membrane surfaces were visually evaluated using digital images; these images were obtained after twenty-four hours of incubation. Triphenyltetrazolium chloride, a biological activity indicator dye, was added to the agar medium (70 mg/l). This dye stained the microorganisms a red color, which facilitated visualization of microbial growth. Agar plating assay results for the zinc-oxide membranes and the uncoated membranes are shown in Figures 4 and 5. Figure 4 shows agar plating assay results of Luria-Bertani agar plates inoculated with *Escherichia coli* after twenty-four hours of incubation and Figure 5 shows agar plating assay results of tryptic soy agar plates inoculated with *Staphylococcus aureus* after twenty-four hours of incubation. Growth of *Escherichia coli* and *Staphylococcus aureus* was inhibited on the zinc oxide-coated membrane surface. A zone of growth inhibition was noted surrounding each zinc oxide-coated membrane, which indicated leaching of zinc oxide from the membrane. There was no discernable difference in antimicrobial activity between membranes studied under either continuous light or dark environments. On the other hand, the uncoated membranes showed no inhibition of *Escherichia coli* or *Staphylococcus aureus* growth under either continuous light or dark environments. Previous work by Akhavan et al. indicated that zinc oxide exhibits antimicrobial activity in both dark and lighted experimental conditions.[28] Zinc oxide exhibits antimicrobial activity against gram negative bacteria and gram positive bacteria; studies by

Liu et al. and Zhang et al. indicate that zinc oxide damages the bacterial cell membrane.[29,30,31] Unlike organic antimicrobial agents, zinc oxide is stable at high temperatures and at high pressures.[32]

Conclusion

Atomic layer deposition is an attractive process for modifying the surfaces of nanoporous alumina membranes and other high aspect ratio nanostructured biomaterials. In this study, zinc oxide-coated 20 nm pore size nanoporous alumina membranes were shown to exhibit activity against *Escherichia coli* and *Staphylococcus aureus* bacteria. Future efforts will involve imcorporating biomimetic selective transport and other "smart" functionalities within the pores of nanoporous alumina membranes using atomic layer deposition-based processes.

Acknowledgments

This document was prepared in conjunction with work accomplished under Contract No. DE-AC09-08SR22470 with the U.S. Department of Energy.

References

1. S. P. Adiga *et al., JOM* **60** (2008), p. 26.
2. F. Keller *et al., J. Electrochem. Soc.* **100** (1953), p. 411.
3. H. Masuda and K. Fukuda, *Science* **268** (1995), p. 1466.
4. G.L. Li *et al., Mod. Phys. Lett. B* **23** (2009), p. 1063.
5. X. Ren *et al., Nanotechnol.* **20** (2009), p. 365604.
6. C.M. Jin *et al., J. Nanosci. Nanotechnol.* **8** (2008), p. 6043.
7. E. Garcia-Cimbrelo *et al., Clin. Orthop. Relat. Res.* **466** (2008), p. 309.
8. M. Lewandowska-Szumiel *et al., Polimery* **42** (1997), p. 195.
9. L.T. Canham *et al., Thin Solid Films* **297** (1997), p. 304.
10. E.J. Anglin *et al., Adv. Drug Deliv. Rev.* **60** (2008), p. 1266.
11. D.W. Gong *et al. Biomed. Microdev.* **5** (2003), p.75.
12. K. Orosz *et al. Mol. Vis.* **10** (2004), p. 555.
13. M. Darder *et al. Thin Solid Films* **49**5 (2006), p. 321.
14. K.E. La Flamme *et al. Biomaterials* **28** (2007), p. 2638.
15. A.C. Attaluri *et al. ASAIO J.* **55** (2009), p. 217.
16. A.H.D. Graham *et al. Biomed. Microdev.* **11** (2009), p. 1091.
17. G. Xiong *et al., J. Phys. Chem. B* **109** (2005), p. 14059.
18. J. J. Wang *et al., J. Vac. Sci. Technol. B* **23** (2005), p. 3209.
19. J. W. Elam *et al., Chem. Mater.* **15** (2003), p. 3507.
20. S. P. Adiga *et al., WIREs Nanomed. Nanobiotechnol.* **1** (2009), p. 568.
21. R. J. Narayan *et al., JOM* **61** (2009), p. 12.
22. J. M. Moon *et al., Biomed. Microdev.* **11** (2009), p. 135.
23. L. Velleman *et al., Microporous Mesoporous Mater.* **126** (2009), p. 87.
24. R. J. Narayan *et al., Phil. Trans. R. Soc. A* **386** (2010), in press.
25. A. Naji and M. F. Harmand, *Biomaterials* **12** (1991), p. 690.
26. D. Chen *et al., Biol. Trace Elem. Res.* **68** (1999), p. 225.
27. R. S.MacDonald, *J. Nutr.* **130** (2000), p. 1500S.
28. O. Akhavan *et al., J. Phys. D* **42** (2009), p. 225305.
29. J. Sawai *et al., J. Chem. Eng. Japan* **28** (1995), p. 288.
30. Y. Le *et al., J. Appl. Microbiol.* **107** (2009), p. 1193.
31. L. L. Zhang *et al., J. Nanoparticle Res.* **9** (2007), p. 479.

32. J. Sawai, *J. Microbiol. Meth.* **54** (2003), p. 177.

Figure Captions

Figure 1. Plan-view scanning electron micrograph obtained from the large pore side of a zinc oxide-coated 20 nm pore size nanoporous alumina membrane.

Figure 2. Twenty-four hour MTT viability assays for the uncoated 20 nm pore size nanoporous alumina membrane and the zinc oxide-coated 20 nm pore size nanoporous alumina membrane. The data was standardized by the uncoated membrane control. The zinc oxide-coated nanoporous alumina membrane demonstrated higher viability than the uncoated nanoporous alumina membrane.

Figure 3. (a) *Staphylococcus aureus* cells on 20 nm pore size uncoated nanoporous alumina membrane. (b) *Staphylococcus aureus* cells on 20 nm pore size zinc oxide-coated nanoporous alumina membrane. (c) *Escherichia coli* cells on 20 nm pore size uncoated nanoporous alumina membrane. (d) *Escherichia coli* cells on 20 nm pore size zinc oxide-coated nanoporous alumina membrane.

Figure 4. Light microscopy images of agar plating assay results. Images were obtained after twenty-four hours of incubation. Zinc oxide-coated 20 nm pore size nanoporous alumina membranes and uncoated 20 nm pore size nanoporous alumina membranes were examined on Luria-Bertani agar plates, which were inoculated with *Escherichia coli*. (a) Uncoated 20 nm pore size nanoporous alumina membrane under continuous light exposure. (b) Zinc oxide-coated 20 nm pore size nanoporous alumina membrane under continuous light exposure. (c) Uncoated 20 nm pore size nanoporous alumina membrane without light exposure. (d) Zinc oxide-coated 20 nm pore size nanoporous alumina membrane without light exposure. An absence of microbial growth was observed on the surfaces of the zinc oxide-coated nanoporous alumina membranes without light exposure and under continuous light exposure. Small zones of inhibition were observed surrounding the zinc oxide-coated nanoporous alumina membranes, indicating release of zinc oxide.

Figure 5. Light microscopy images of agar plating assay results. Images were obtained after twenty-four hours of incubation. Zinc oxide-coated 20 nm pore size nanoporous alumina membranes and uncoated 20 nm pore size nanoporous alumina membranes were examined on tryptic soy agar plates, which were inoculated with *Staphylococcus aureus*. (a) Uncoated 20 nm pore size nanoporous alumina membrane under continuous light exposure. (b) Zinc oxide-coated 20 nm pore size nanoporous alumina membrane under continuous light exposure. (c) Uncoated 20 nm pore size nanoporous alumina membrane without light exposure. (d) Zinc oxide-

coated 20 nm pore size nanoporous alumina membrane without light exposure. An absence of microbial growth was observed on the surfaces of the zinc oxide-coated nanoporous alumina membranes without light exposure and under continuous light exposure. Small zones of inhibition were observed surrounding the zinc oxide-coated nanoporous alumina membranes, indicating release of zinc oxide.

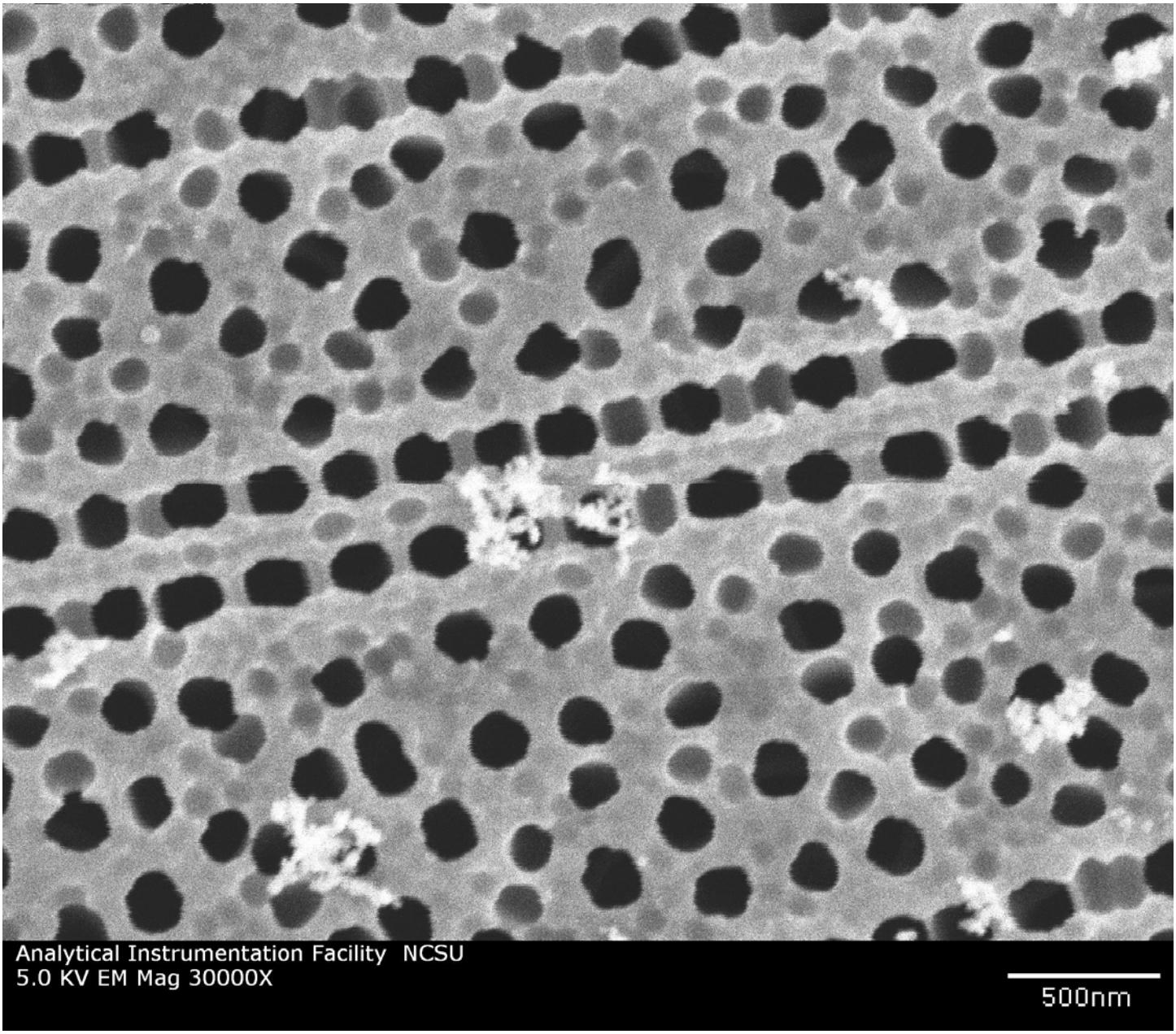
Analytical Instrumentation Facility NCSU
5.0 KV EM Mag 30000X
500nm

Figure 1

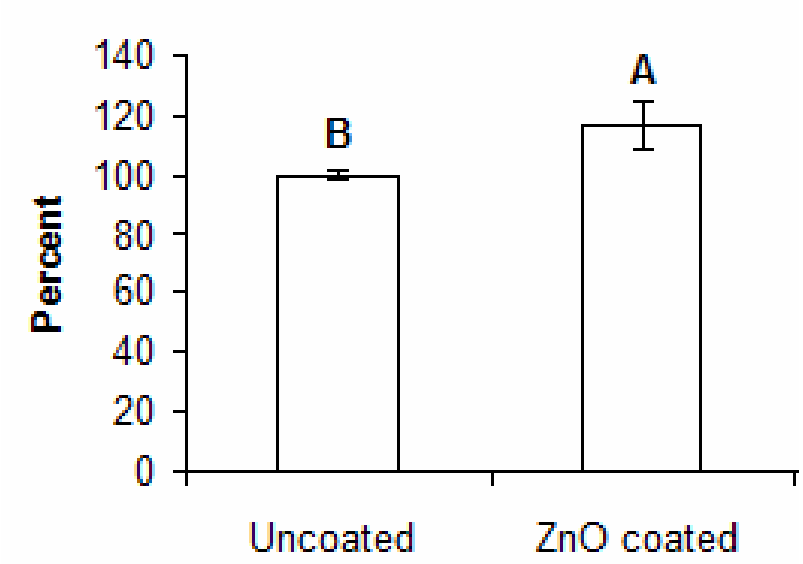

Figure 2

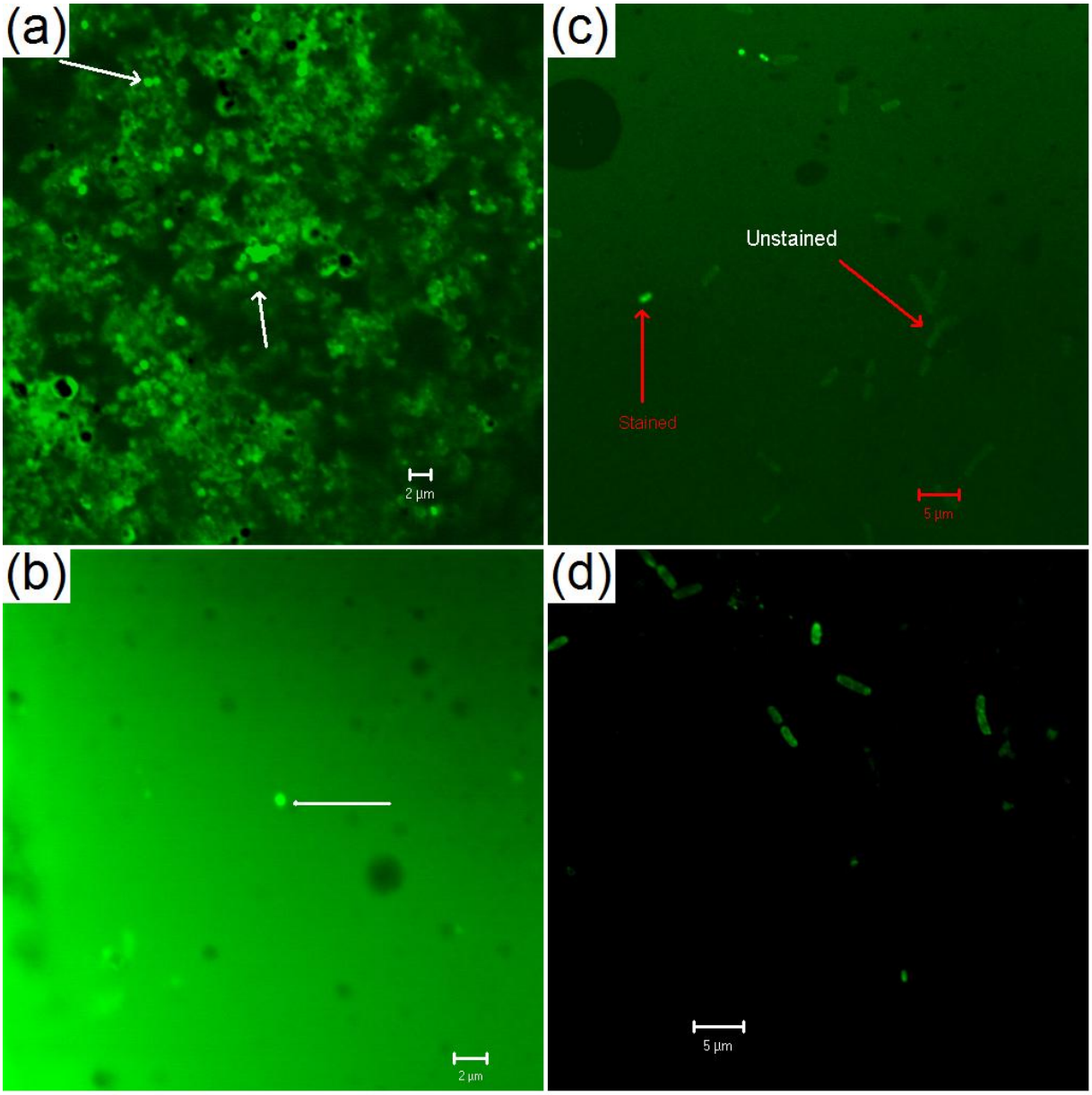

Figure 3

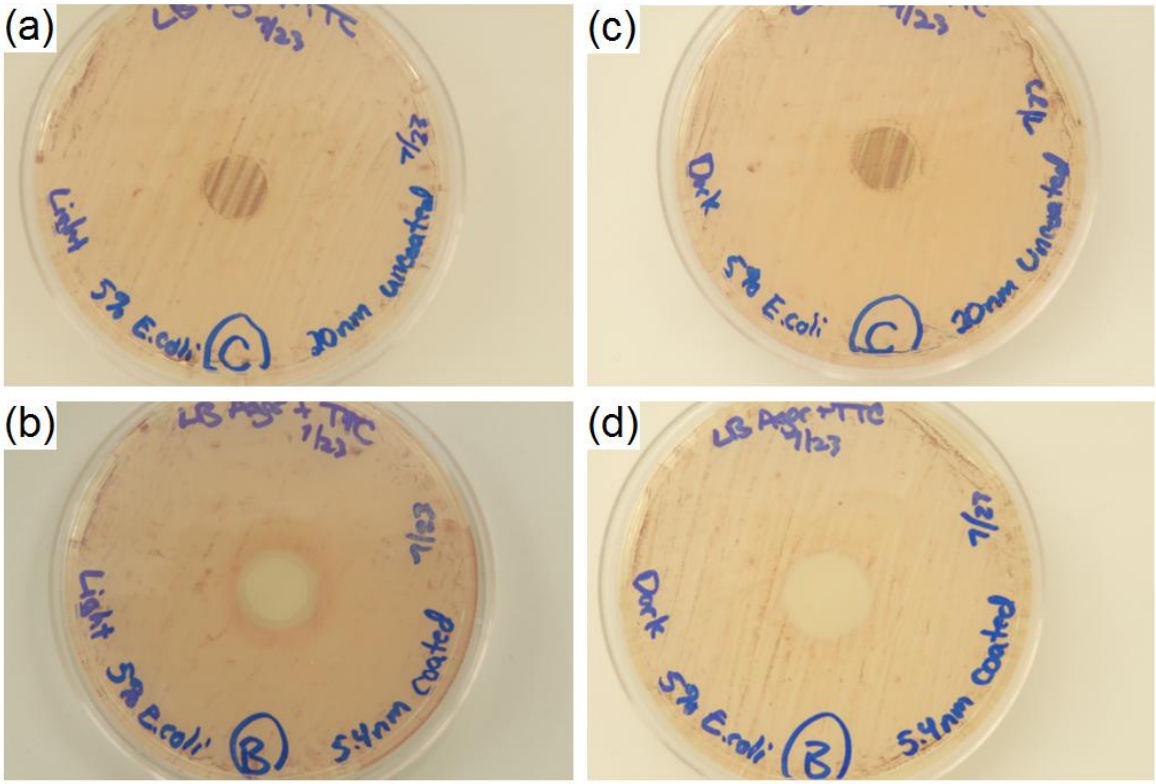
(a)
(c)
(b)
(d)
Light
5% E.coli
C
20nm Uncoated
7/23
Dark
5% E.coli
C
20nm Uncoated
7/23
Light
5% E.coli
B
5.4nm Coated
7/23
Dark
5% E.coli
B
5.4nm Coated
7/23

Figure 4

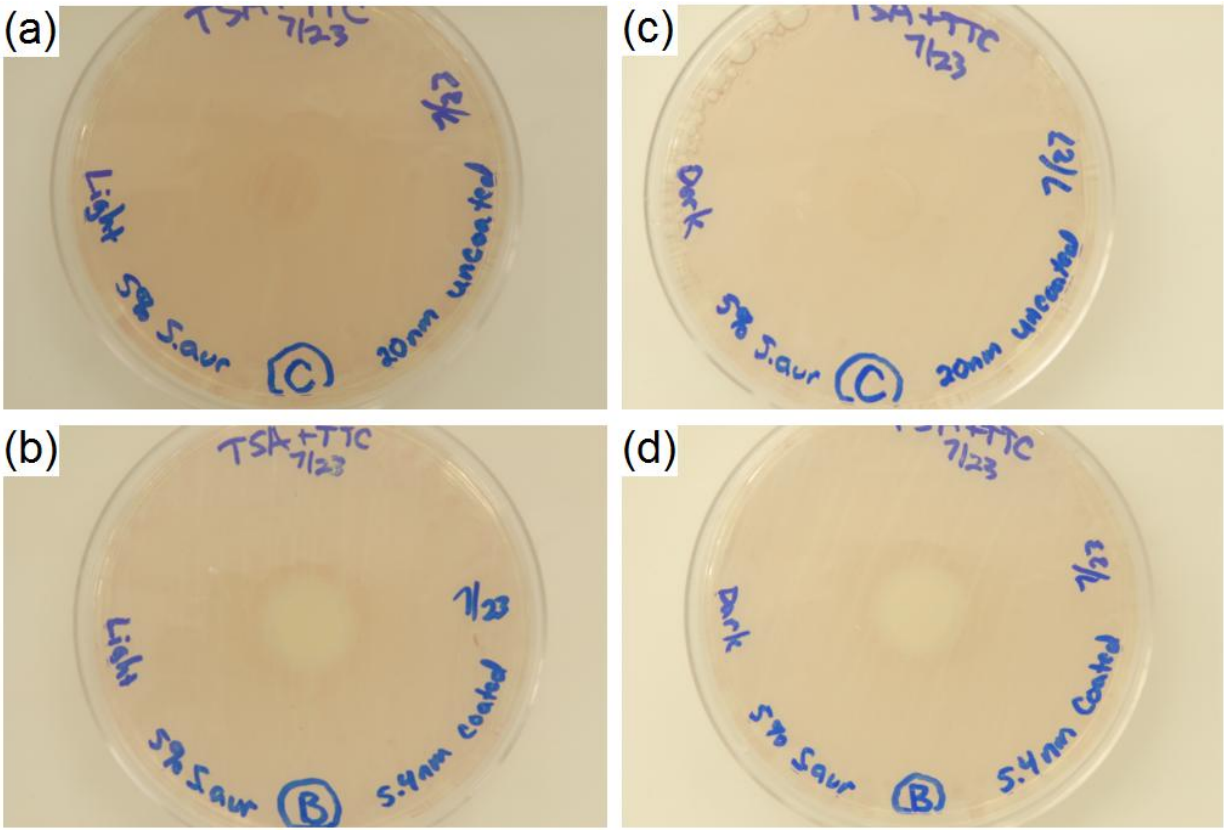
(a)
(c)
(b)
(d)
TSA+TTC
7/23
Light
Dark
5% S.aur
20nm uncoated
5.4nm coated
(C)
(B)

Figure 5